Eur. Phys. J. Special Topics **226**, 849–855 (2017)

DOI: 10.1140/epjst/e2016-60187-0

THE EUROPEAN PHYSICAL JOURNAL SPECIAL TOPICS

Regular Article

A new polymorph of 4′-hydroxyvalerophenone revealed by thermoanalytical and X-ray diffraction studies

Cátia S.D. Lopes[1], Carlos E.S. Bernardes[1], M. Fátima M. Piedade[1,2], Hermínio P. Diogo[2], and Manuel E. Minas da Piedade[1,a]

[1] Centro de Química e Bioquímica e Departamento de Química e Bioquímica, Faculdade de Ciências, Universidade de Lisboa, 1649-016 Lisboa, Portugal
[2] Centro de Química Estrutural, Instituto Superior Técnico, Universidade de Lisboa, 1049-001 Lisboa, Portugal

Received 27 July 2016 / Received in final form 18 October 2016
Published online 18 April 2017

Abstract. A new polymorph of 1-(4-hydroxyphenyl)pentan-1-one (4′-hydroxyvalerophenone, HVP) was identified by using differential scanning calorimetry, hot stage microscopy, and X-ray powder diffraction. This novel crystal form (form II) was obtained by crystallization from melt. It has a fusion temperature of $T_{fus} = 324.3 \pm 0.2$ K and an enthalpy of fusion $\Delta_{fus}H^{o}_{m} = 18.14 \pm 0.18\,kJ \cdot mol^{-1}$. These values are significantly lower than those observed for the previously known phase (form I, monoclinic, space group $P2_1/c$, $T_{fus} = 335.6 \pm 0.7$ K; $\Delta_{fus}H^{o}_{m} = 26.67 \pm 0.04\,kJ \cdot mol^{-1}$), which can be prepared by crystallization from ethanol. The results here obtained, therefore, suggest that form I is thermodynamically more stable than the newly identified form II and, furthermore, that the two polymorphs are monotropically related.

1 Introduction

Systematic studies of polymorphism using families of organic crystals where the different building blocks are structurally related molecules are particularly interesting to understand how the interplay of molecular size, shape and types of interaction may affect the packing architecture and the relative stability of crystal forms. One such family is that of $HOC_6H_4C(O)R$ (R = H, *n*-alkyl) compounds, which contain a common $HOC_6H_4C(O)$ fragment, and differ in the length of the *n*-alkyl chain bonded to the carbonyl group.

Up to now polymorphism has only been reported for 4-hydroxybenzaldehyde (HBA; R = H; cr I [1] and cr II [2] forms) and 4'-hydroxyacetophenone (HAP, R = CH_3; cr I [3] and cr II [3–6] forms). The latter compound also forms hydrates [7,8] and exhibits unique features in terms of crystallization from water, since depending on the selected concentration range, the formation of either a hydrate or an anhydrous phase can be mediated by an emulsion [7,9]. All these results suggest

[a] e-mail: memp@fc.ul.pt

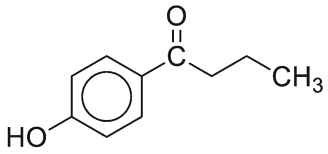

Fig. 1. Molecular structure of 4′-hydroxyvalerophenone (HVP).

that other members of the $HOC_6H_4C(O)R$ family should be prone to polymorphism, albeit only one crystal form has been reported for either 4′-hydroxybutyrophenone (HBP; R = C_3H_7) [10] and 4′-hydroxyvalerophenone (HVP; R = C_4H_9) [11]. No other crystal structures are known for $HOC_6H_4C(O)R$ compounds [12].

Differential scanning calorimetry (DSC) has been an invaluable tool for the detection of polymorphism in molecular organic crystals and for the definition of their stability domains and elucidation of monoptropic/enantiotropic relationships [13–16]. In this work evidence for a new polymorph of 4′-hydroxyvalerophenone (HVP, Fig. 1) is presented, based on DSC studies supplemented by hot stage microscopy and X-ray powder diffraction experiments. These studies also suggest a monotropic relationship between this new HVP phase and the previously known one (monoclinic, space group $P2_1/c$, here dubbed form I) [11,12].

2 Materials and methods

2.1 Sample

The HVP used as starting material for the polymorphism studies was the same previously employed in enthalpy of vaporization/sublimation measurements [17], which had been obtained by crystallization from ethanol. The molar fraction purity given by HPLC-ESI/MS analysis was 0.99999. Indexation of the powder pattern recorded at 297 ± 1 K indicated that the material corresponded to the monoclinic HVP phase (space group $P2_1/c$; $a = 9.990 \pm 0.002$ Å, $b = 10.454 \pm 0.002$ Å, $c = 9.882 \pm 0.002$ Å, $\beta = 107.46 \pm 0.03°$) previously characterized by single crystal X-ray diffraction [11,12].

2.2 Differential scanning calorimetry (DSC)

DSC scans in the range 153 K to 453 K were carried out with a TA Instruments 2920 MTDSC apparatus equipped with a refrigerated cooling accessory (LNCA) that provided automatic and continuous programmed sample cooling down to 123 K. The samples with a mass of ∼5.0 mg were sealed under air in aluminum pans. All the measurements were done under Helium (Air Liquide N55) at a flow rate of $30\,cm^3 \cdot min^{-1}$, using a heating rate of $10\,K \cdot min^{-1}$. Calibration of the temperature scale of the instrument was based on the temperatures of fusion, T_{fus}, of *n*-decane ($T_{fus} = 243.75$ K), *n*-octadecane ($T_{fus} = 301.77$ K), hexatriacontane ($T_{fus} = 347.30$ K), indium ($T_{fus} = 430.61$ K), and tin ($T_{fus} = 506.03$ K). The heat flow scale was calibrated by using indium ($\Delta_{fus}h = 28.71\,J \cdot g^{-1}$). All weightings were performed with a precision of $\pm 0.1\,\mu g$ in a Mettler UMT2 ultra-micro balance. Note, finally, that the uncertainties assigned to the onset and maximum temperatures of the fusion or crystallization peaks and to the corresponding enthalpies reported in this work correspond to twice the standard error of the mean of five independent determinations. Furthermore, the molar enthalpy values are based on a molar mass of HVP,

$M(C_{11}H_{14}O_2) = 178.231\,g \cdot mol^{-1}$, calculated from the conventional atomic masses recommended by the IUPAC Commission in 2013 [18].

2.3 Hot stage microscopy (HSM)

Hot stage polarized optical microscopy studies were performed with an Olympus BX51 microscope equipped with a Linkam LTS360 liquid nitrogen-cooled cryostage and a Linkam TMS94 programmable temperature controller. The microstructure of the sample was monitored by taking microphotographs with an Olympus C5060 wide zoom camera. Images were recorded at selected temperatures with 250× or 500× magnification. The HVP sample was placed between two microscope slides and inserted into the hot stage. It was then subjected to the following temperature program analogous to that used in the DSC experiments (heating/cooling rate: $10\,K{\cdot}min^{-1}$): (*i*) cooling from 298 K to 173 K; (*ii*) heating to 393 K; (*iii*) cooling of isotropic liquid to 263 K; (*iv*) heating of the crystallized material to 353 K.

2.4 X-ray powder diffraction (XRPD)

X-ray powder diffraction (XRPD) patterns were collected at 297 ± 1 K, on a D8 Advance Bruker X-ray diffractometer operating in the $\theta - 2\theta$ mode. The apparatus was equipped with a LinxEye detector and a Ni-filtered Cu-Kα ($\lambda = 1.5406$ Å) radiation source. The radiation source amperage and voltage were 40 kV and 40 mA, respectively. Diffraction data were collected in the 2θ range from 7° to 35°, in 0.02° steps, and with an overall scan time of approximately 15 min. The samples were mounted on a glass sample holder. The program MERCURY 3.026 [19] was used to simulate diffraction patterns from published single crystal X-ray diffraction data.

3 Results and discussion

The first evidence of a new HVP polymorph was provided by DSC experiments carried out in the temperature range 153 K to 453 K, using the form I (monoclinic, $P2_1/c$) sample produced by crystallization from ethanol. Figure 2 shows that when this material was cooled from ambient temperature (296 ± 2 K) to 153 K and then heated at $10\,K \cdot min^{-1}$ to 453 K only an endothermic peak corresponding to fusion was detected with onset (taken as the fusion temperature in this work) at $T_{fus} = 335.6 \pm 0.7$ K, maximum at $T_{max} = 337.9 \pm 0.4$ K, and molar enthalpy of fusion, $\Delta_{fus}H_m = 26.67 \pm 0.04\,kJ \cdot mol^{-1}$.

Subsequent cooling of the sample from the isotropic liquid, at $10\,K{\cdot}min^{-1}$, revealed an exothermic peak with $T_{cryst} = 308.8 \pm 1.6$ K, $T_{max} = 303.9 \pm 3.0$ K and with an enthalpy $\Delta_{cryst}H_m = -(16.68 \pm 0.84)\,kJ \cdot mol^{-1}$. The cross polarized HSM images in Figures 3a to 3c clearly indicated that this peak corresponds to the crystallization of HVP, and that the process occurs between 303 K and 298 K in good agreement with the DSC results. No thermal event was observed upon further cooling of crystallized HVP to 212 K.

Heating the crystallized material from 212 K to 353 K, at the same heating rate, showed only one endothermic peak with $T_{fus} = 324.3 \pm 0.2$ K, $T_{max} = 327.6 \pm 0.6$ K, and $\Delta_{fus}H_m = 18.14 \pm 0.18\,kJ \cdot mol^{-1}$. Confirmation that this peak corresponded indeed to a fusion event was provided by the results of HSM experiments illustrated in Figure 3d and 3e. The HSM observations also indicated that fusion occurs in the 323 K

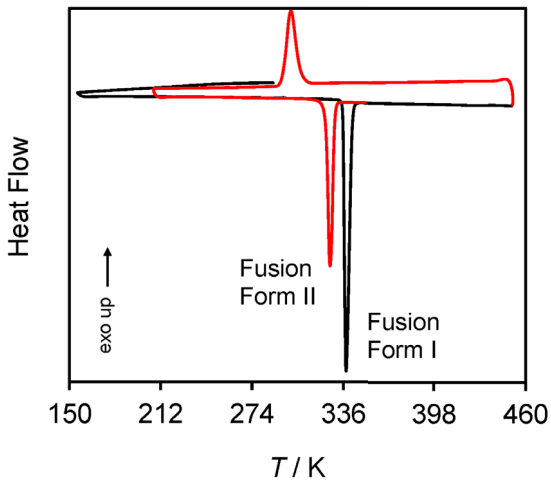

Fig. 2. Results of DSC experiments carried out on HVP in the range 153 K to 453 K, at a rate of $10\,\mathrm{K}\cdot\mathrm{min}^{-1}$. The black line corresponds to the cooling of the initial sample from 298 K to 153 K, followed by heating to 453 K. The red line refers to cooling the isotropic liquid from 453 K to 212 K, followed by heating the crystallized phase to 353 K.

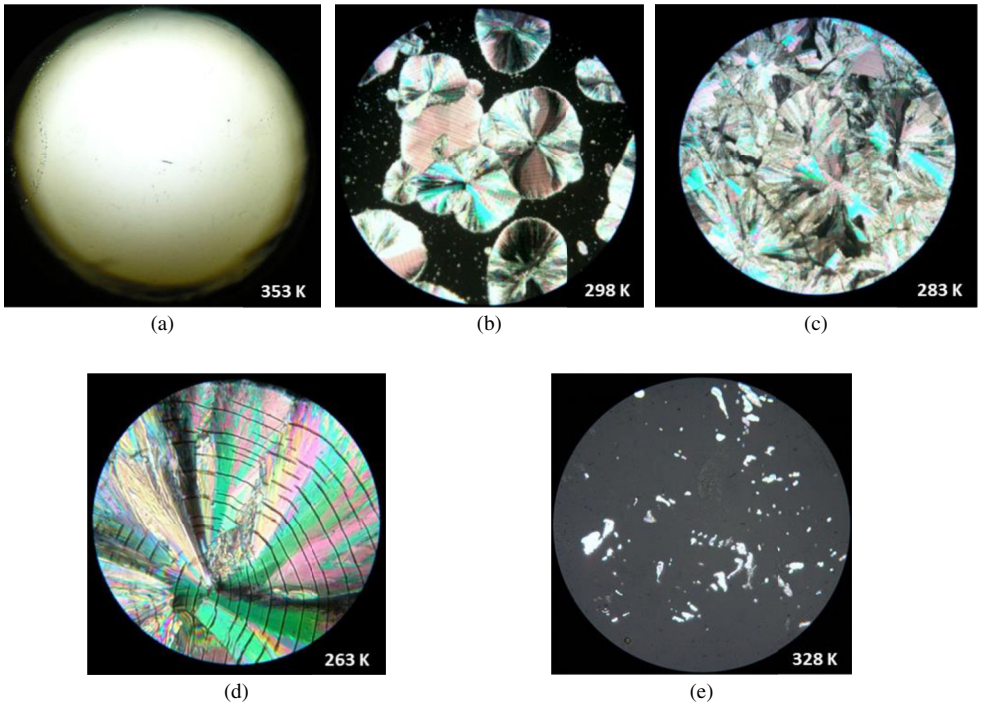

(a) (b) (c)

(d) (e)

Fig. 3. Hot stage polarized optical microscopy images showing the crystallization of the new HVP polymorph (form II) from melt and its subsequent fusion on heating: (a) isotropic liquid at 353 K (250×); (b) initial stages of crystallization at 298 K (250×); (c) the material at 283 K, after complete crystallization (250×); (d) form II further cooled to 263 K (500×); (e) form II undergoing melting at ∼328 K, after being heated from 263 K (500×).

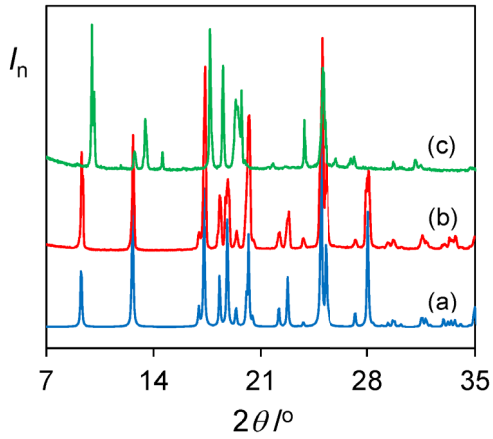

Fig. 4. Comparison of the X-ray powder diffraction (XRPD) patterns of HVP: (a) simulated from single crystal X-ray diffraction data previously reported by Luo et al. [11,12] (form I) (b) obtained for the starting material of the DSC and HSM experiments (form I); (c) recorded for the material crystallized from the melt (form II). The intensities of the powder patterns were normalized (I_n) relative to that of the most intense peak.

to 329 K range in agreement with the DSC findings. The large differences in temperature ($\Delta T_{\text{fus}} = 11.2\,\text{K}$) and enthalpy of fusion ($\Delta\Delta_{\text{fus}}H_{\text{m}} = 8.5\,\text{kJ}\cdot\text{mol}^{-1}$) between the starting material (crystallized from ethanol) and the material crystallized from the melt strongly suggested that the latter corresponds to a new polymorphic form of HVP (form II). It should be pointed out that no sample decomposition was noted when the sealed DSC crucibles were opened after completion of the heating/cooling cycle shown in Figure 2. Furthermore, when an unsealed DSC crucible was used, the detected mass variation at the end of the experiment was smaller than 0.08%. Note, finally, that no particular significance can be attributed to the difference between the mean values of the enthalpies of crystallization ($\Delta_{\text{cryst}}H_{\text{m}} = -16.68 \pm 0.84\,\text{kJ}\cdot\text{mol}^{-1}$) and fusion ($\Delta_{\text{fus}}H_{\text{m}} = 18.14 \pm 0.18\,\text{kJ}\cdot\text{mol}^{-1}$) of form II, since no evidence for a glass transition has been found and the $\Delta_{\text{cryst}}H_{\text{m}}$ results obtained in the five individual runs span a range (15.7–18.1 $\text{kJ}\cdot\text{mol}^{-1}$) that covers $\Delta_{\text{fus}}H_{\text{m}}$ when the uncertainty interval is considered.

The conclusion that a new HVP polymorph (form II) had been found was further confirmed by X-ray powder diffraction experiments. Figure 4 shows a comparison of three XRPD patterns corresponding to HVP: (a) simulated from single crystal data previously reported for form I (monoclinic, space group $P2_1/c$, $Z'/Z = {}^1/_4$; $a = 9.990 \pm 0.002$ Å, $b = 10.454 \pm 0.002$ Å, $c = 9.882 \pm 0.002$ Å, $\beta = 107.46 \pm 0.03°$) at 298 ± 5 K [11,12]; (b) obtained at 297 ± 1 K for the starting material of the DSC and HSM experiments; and (c) recorded at 297 ± 1 K for the material crystallized from the melt. Figure 4 clearly shows that while the XRPD pattern of the starting material (curve b) matches that simulated for form I (curve a) the same is not true for the material crystallized from the melt (curve c), which should therefore correspond to a different HVP polymorph (form II). Efforts to obtain crystals suitable for a structural determination by single crystal X-ray diffraction are currently under way.

Finally, the results of the DSC experiments discussed above, indicate that the HVP polymorph with the higher temperature of fusion (form I) has also the higher enthalpy of fusion. Based on Burger and Ramberger's heat of fusion rule [20], this suggests a monotropic relationship between the two HVP forms or, in other words, that form I is more stable than form II at any temperature before fusion. Such

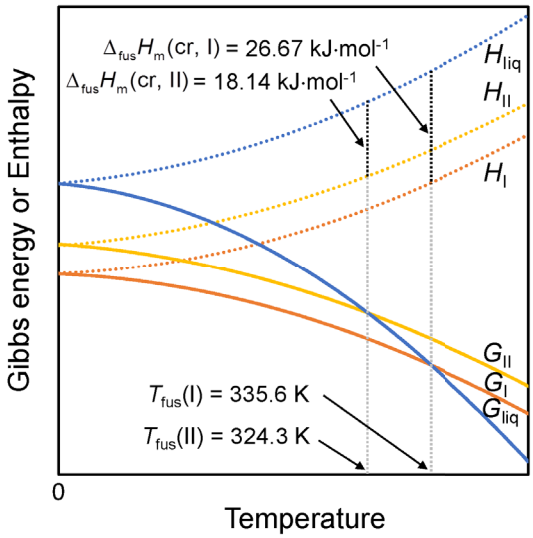

Fig. 5. Schematic representation of the Gibbs energy and enthalpy versus temperature phase diagram highlighting the monotropic nature of the HVP polymorphic system.

relationship can be illustrated by means of the qualitative Gibbs energy and enthalpy versus temperature phase diagram shown in Figure 5. A quantitative drawing of this type of plot requires a variety of auxiliary data that is currently unavailable (e.g. heat capacities, enthalpies of formation and entropies of the different phases) [3,21]. The diagram in Figure 5 relies on the following considerations: (*i*) the difference between the heat capacity of the two polymorphs is approximately constant; (*ii*) at 0 K $G = H - TS = H$; (*iii*) at the fusion temperatures of forms II ($T_{\mathrm{fus}} = 324.3 \pm 0.2\,\mathrm{K}$) and I ($T_{\mathrm{fus}} = 335.6 \pm 0.7\,\mathrm{K}$) the Gibbs energy of the liquid phase equals that of the solid form being examined; (*iv*) under the same conditions, the enthalpy differences between the liquidus line and the solidus lines for forms II and I are given by the corresponding enthalpies of fusion, $\Delta_{\mathrm{fus}}H_{\mathrm{m}}(\mathrm{cr,II}) = 18.14 \pm 0.18\,\mathrm{kJ \cdot mol^{-1}}$ and $\Delta_{\mathrm{fus}}H_{\mathrm{m}}(\mathrm{cr,\ I}) = 26.67 \pm 0.04\,\mathrm{kJ \cdot mol^{-1}}$, respectively. As shown in Figure 5 the Gibbs energy curves of forms I and II do not cross before fusion. This is the hallmark of a monotropic relationship, where one polymorph is always thermodynamically more stable that the other along the full solid state domain.

This work was supported by FCT, Portugal, through Projects PEst-OE/QUI/UI0612/2013 and PEst-OE/QUI/UI0100/2013, and a post-doctoral grant awarded to C.E.S. Bernardes (SFRH/BPD/101505/2014). We also acknowledge the COST action CM1402.

References

1. F. Iwasaki, Acta Crystallogr. **B33**, 1646 (1977)
2. J.P. Jasinski, R.J. Butcher, B. Narayana, M.T. Swany, H.S. Yathirajan, Acta Crystallogr. **E64**, o187 (2008)
3. C.E.S. Bernardes, M.F.M. Piedade, M.E. Minas da Piedade, Cryst. Growth Des. **8**, 2419 (2008)
4. B.K. Vainshtein, G.M. Lobanova, G.V. Gurskaya, Kristallografiya **19**, 531 (1974)
5. S. Chenthamarai, D. Jayaraman, K. Meera, P. Santhanaraghavan, C. Subramanian, G. Bocelli, P. Ramasamy, Crystal Eng. **4**, 37 (2001)

6. A.J. Kresge, A.J. Lough, Y. Zhu, Acta Crystallogr. **58**, o1057 (2002)
7. C.E.S. Bernardes, M.E. Minas da Piedade, Cryst. Growth Des. **12**, 2932 (2012)
8. C.E.S. Bernardes, M.F.M. Piedade, M.E. Minas da Piedade, Cryst. Growth Des. **10**, 3070 (2010)
9. C.E.S. Bernardes, M.L.S. Matos Lopes, J.R. Ascenso, M.E. Minas da Piedade, Cryst. Growth Des. **14**, 5436 (2014)
10. B. Xu, Z.Q. Feng, J.T. Wang, L.G. Hu, J. Huang, Acta Crystallogr. **E62**, O2603 (2006)
11. Z.H. Luo, H.J. Zhu, S. Liu, Acta Crystallogr. **E62**, O5054 (2006)
12. F.H. Allen, Acta Crystallogr. **B58**, 380 (2002)
13. J. Bernstein, *Polymorphism in Molecular Crystals* (Oxford University Press, Oxford, 2002)
14. H.G. Brittain, *Polymorphism in Pharmaceutical Solids* (Marcel Dekker, New York, 1999)
15. H.G. Brittain, J. Pharm. Sci. **96**, 705 (2007)
16. R. Hilfiker, *Polymorphism in the Pharmaceutical Industry* (Wiley-VCH Verlag GmbH & Co., Weinheim, 2006)
17. C.S.D. Lopes, F. Agapito, C.E.S. Bernardes, M.E. Minas da Piedade, J. Chem. Thermodyn. **104**, 281 (2017)
18. J. Meija, T.B. Coplen, M. Berglund, W.A. Brand, P. De Bièvre, M. Gröning, N.E. Holden, J. Irrgeher, R.D. Loss, T. Walczyk, T. Prohaska, Pure Appl. Chem. **88**, 265 (2016)
19. C.F. Macrae, I.J. Bruno, J.A. Chisholm, P.R. Edgington, P. McCabe, E. Pidcock, L. Rodriguez-Monge, R. Taylor, J. van de Streek, P.A. Wood, J. Appl. Crystallogr. **41**, 466 (2008)
20. A. Burger, R. Ramberger, Mikrochim. Acta **2**, 259 (1979)
21. R.G. Simões, C.E.S. Bernardes, M.E. Minas da Piedade, Cryst. Growth Des. **13**, 2803 (2013)